Materials Science and Engineering C 56 (2015) 511–517

Contents lists available at ScienceDirect

Materials Science and Engineering C

journal homepage: www.elsevier.com/locate/msec

Electrospun nanofibrous scaffolds of segmented polyurethanes based on PEG, PLLA and PTMC blocks: Physico-chemical properties and morphology

Rafael Bergamo Trinca [a], Gustavo A. Abraham [b], Maria Isabel Felisberti [a,*]

[a] Institute of Chemistry, University of Campinas (UNICAMP), P.O. Box 6154, Zip Code 13083-970 Campinas, SP, Brazil
[b] Research Institute for Materials Science and Technology INTEMA (UNMdP-CONICET), Av. Juan B. Justo 4302, B7608FDQ Mar del Plata, Argentina

ARTICLE INFO

Article history:
Received 8 January 2015
Received in revised form 14 May 2015
Accepted 10 July 2015
Available online 16 July 2015

Keywords:
Electrospinning
Electrospun scaffold
Segmented polyurethanes
Microstructure

ABSTRACT

Biocompatible polymeric scaffolds are crucial for successful tissue engineering. Biomedical segmented polyurethanes (SPUs) are an important and versatile class of polymers characterized by a broad spectrum of compositions, molecular architectures, properties and applications. Although SPUs are versatile materials that can be designed by different routes to cover a wide range of properties, they have been infrequently used for the preparation of electrospun nanofibrous scaffolds. This study reports the preparation of new electrospun polyurethane scaffolds. The segmented polyurethanes were synthesized using low molar masses macrodyols (poly(ethylene glycol), poly(L-lactide) and poly(trimethylene carbonate)) and 1,6-hexane diisocyanate and 1,4-butanodiol as isocyanate and chain extensor, respectively. Different electrospinning parameters such as solution properties and processing conditions were evaluated to achieve smooth, uniform bead-free fibers. Electrospun micro/nanofibrous structures with mean fiber diameters ranging from 600 nm to 770 nm were obtained by varying the processing conditions. They were characterized in terms of thermal and dynamical mechanical properties, swelling degree and morphology. The elastomeric polyurethane scaffolds exhibit interesting properties that could be appropriate as biomimetic matrices for soft tissue engineering applications.

1. Introduction

The development of biocompatible polymeric scaffolds for tissue engineering applications still poses a huge challenge. Many techniques to prepare highly porous scaffolds have been developed and explored in recent years [1]. Electrospinning is an emerging technology that can be used to produce micro/nanofibrous scaffolds for a wide range of biomedical applications such as drug delivery, wound dressings, vascular grafts, and tissue engineering matrices [2–4]. Nanofiber-based scaffolds prepared by electrospinning biodegradable synthetic polymers not only mimic the micro/nanoscale structure of the natural extracellular matrix but also its spatial organization on the mesoscopic scale (control over fiber orientation and spatial placement) [5].

Electrospun matrices can be obtained from a broad variety of materials, including both synthetic and natural polymers, ceramics and polymer/ceramic composites. Fibers with diameters in the range from several micrometers to less than 100 nm can be produced. The resulting fibrous scaffolds have high surface area-to-volume ratios, high porosity and an interconnected pore structure.

Synthetic biodegradable polymers, especially biomedical polyesters such as poly(lactic acid), poly(glycolic acid), poly(ε-caprolactone), polyhydroxybutyrate, blends, composites and block copolymers, have been widely used to produce nanofibers. These scaffolds were investigated for tissue engineering applications in bone, cartilage, muscle, tendon, nerve, myocardial, bladder, and wound dressings [6].

The chemistry of polyurethanes allows preparing materials with controlled physico-chemical, mechanical, and biodegradation properties that can be achieved through the appropriate selection of monomers and their ratio. Segmented polyurethanes (SPU) have been infrequently used for the fabrication of electrospun nanofibrous scaffolds.

Biodegradation of SPU to non-toxic components may be promoted by the use of aliphatic diisocyanates and degradable chain extenders. Moreover, there is an increasing need for elastomeric synthetic biodegradable materials that mimic soft tissue properties. Typical polyesters and copolyesters, such as those based on lactic and glycolic acids, are relatively stiff, nonelastic materials and are not ideally suited for the engineering of soft, flexible tissues such as cardiovascular, urological, or gastrointestinal tissues. In recent years, novel biocompatible and biodegradable SPU elastomers have been investigated [7]. Applications of SPU in cardiovascular tissue engineering such as bone, muscle, and nerve regeneration have been investigated [8–11].

* Corresponding author.
E-mail addresses: rafaeltrinca@gmail.com (R.B. Trinca), gabraham@fi.mdp.edu.ar (G.A. Abraham), misabel@iqm.unicamp.br (M.I. Felisberti).

http://dx.doi.org/10.1016/j.msec.2015.07.018
0928-4931/

In recent years, few works on electrospun polyurethane scaffolds have been published [12–14]. Henry et al. [15] reported that highly porous electrospun polyurethane scaffolds exhibited a superior host tissue and angiogenic response compared to polyurethane membranes or films. Caracciolo et al. [16,17] reported the preparation, characterization, thermal and mechanical properties, and in vitro biological properties of aliphatic segmented poly(ester urethane)s based on poly(ε-caprolactone) (PCL), 1,6-hexamethylene diisocyanate and novel aliphatic and aromatic chain extenders containing urea or ester functional groups. Solution properties and processing parameters were optimized to achieve uniform bead-free fibers, and the influence of the experimental processing conditions on the fiber morphology was investigated [18]. The thermal behavior indicated that the chemical structure of hard segments and the processing conditions resulted in the phase separation of nanofibrous SPU into soft and hard domains, and the fibrous morphology influenced the water absorption and hydrolytic degradation rate [19].

In this work, two SPU formulations based on poly(ethylene glycol), poly(L-lactide) and poly(trimethylene carbonate) blocks (PEG, PLLA and PTMC, respectively) were studied for electrospinnability into fibrous scaffolds. These two polymers differ in their PLLA and PTMC mass ratios, while maintaining the same PEG content. To optimize the conditions to create SPU nanofibers, parameters of the electrospinning process such as polymer concentration, applied voltage, needle tip-to-collector distance and flow rate were varied to achieve smooth, uniform bead-free fibers. Scaffolds were characterized in terms of thermal properties, dynamical mechanical properties, contact angle, swelling degree and morphology.

2. Experimental section

2.1. Materials

Poly(ethylene glycol) (PEG) (3.0 kDa), poly(L-lactide) (PLLA) (5.3 kDa) and poly(trimethylene carbonate) (PTMC) (3.7 kDa) were used as macrodiols. 1,6-Hexane diisocyanate (HDI) and 1,4-butanediol were purchased from Sigma Aldrich, Germany. Chloroform, dichloromethane and *N*,*N*-dimethylformamide were acquired from Synth (Brazil) and used as received. Toluene was dried by stirring with calcium chloride followed by filtration and distillation in the presence of metallic sodium.

2.2. SPU synthesis

Two SPUs based on PEG, PLLA, and PTMC were synthesized. First, PLLA and PTMC homopolymers were obtained by ring-opening polymerization reactions from L-lactide and trimethylene carbonate monomers (purchased from Sigma Aldrich and Boehringer Ingelheim, respectively), using 1,4-butanediol as an initiator [20]. SPUs were synthesized as previously reported via a standard two-step polymerization [21]. Briefly, PEG, PLLA and PTMC macrodiols in a desired ratio were reacted with HDI at 40 °C in a toluene solution. Pre-polymer chain extension was performed by using 1,4-butanediol. Table 1 summarizes the compositions and molar masses of the synthesized SPUs. SPUs were named according to the macrodiol weight percent as SPU-1 (PEG 10%, PLLA 60% and PTMC 30%) and SPU-2 (PEG 10%, PLLA 45% and PTMC 45%).

Table 1
Compositions of synthesized SPUs.

	Reaction medium (mass fraction)			SPU composition * (mass fraction)			Molar mass (kDa)		
Sample	PEG	PLLA	PTMC	PEG	PLLA	PTMC	M_n	M_w	M_w/M_n
PEG	–	–	–	–	–	–	3.0	3.1	1.03
PLLA	–	–	–	–	–	–	5.3	6.1	1.16
PTMC	–	–	–	–	–	–	3.7	6.9	1.8
SPU-1	0.10	0.60	0.30	0.11	0.58	0.31	68	151	2.2
SPU-2	0.10	0.45	0.45	0.11	0.42	0.47	102	173	1.7

* ^{1}H NMR.

2.3. Film preparation

SPU films were obtained by a typical solution-casting technique from SPU solutions in chloroform. After solvent evaporation, samples were heated up to 70 °C for 1 h, cooled to 40 °C and then exhaustively dried under vacuum.

2.4. SPU electrospun scaffold preparation

SPU nanofibrous scaffolds were prepared by an electrospinning technique. SPU solutions (10–12% wt) were obtained by dissolving SPU in a dichloromethane/dimethylformamide solvent mixture (DCM/DMF 60:40 volume ratio) under magnetic stirring. Each solution was loaded into a standard 10 mL plastic syringe connected to a polyamide tube, with a blunt 18-gauge stainless steel needle (Aldrich Chemical Co.) attached to the open end as a nozzle. The flow rate was controlled by using a programmable syringe pump (Activa A22 ADOX S.A., Argentina). A high-voltage power source (ES30P, Gamma High Voltage Research Inc., Ormond Beach, FL) was used to charge the solution by attaching the emitting electrode of positive polarity to the nozzle and the grounding electrode to the aluminum collector plate. All experiments were carried out at room temperature and a relative humidity of 50% in a chamber having a ventilation system.

Electrospun scaffolds were obtained after setting the conditions summarized in Table 2. All samples were collected over 50 min. The electrospun scaffolds were dried overnight under vacuum at room temperature to fully eliminate the residual solvent and then stored in a desiccator until testing.

2.5. Methods

2.5.1. SPU characterization

The ^{1}H NMR spectra of the polymer solutions (20 mg in 0.6 mL $CDCl_3$) were obtained using a Bruker Avance III 500 MHz Spectrometer (operating at 25 °C, 11.7 T, pulse delay of 1 s, acquisition time of 1.6 s, 128 scans with 32 k points and an FID resolution of 0.3 Hz).

Gel permeation chromatography (GPC) was performed on a Viscotek GPCmax VE 2001 chromatograph equipped with a Viscotek VE 3580 RI Detector, a Viscotek UV Detector 2500, a Viscotek TGuard 10 × 4.6 mm guard column, and 3 Shodex KF-806 M columns. The column system was kept at 40 °C. Anhydrous tetrahydrofuran (Tedia, HPLC grade) was used as an eluent at a flow rate of 1.0 mL min^{-1}, as well to prepare polymer solutions of 8.0 mg mL^{-1} (injection volume of 100 μL). Molar masses are relative to polystyrene (PS) standards (Viscotek) with molar masses from 1050 to 3,800,000 g mol^{-1}.

The thermal properties of SPU films and scaffolds were studied using differential scanning calorimetry (DSC) and dynamic-mechanical thermal analysis (DMTA). DSC was performed on a Q2000 DSC (TA Instruments) operating with a heating rate of 10 °C min^{-1} in an argon

Table 2
Experimental conditions used for electrospinning SPU solutions and mean fiber diameters of prepared samples (DCM/DMF 60/40).

Sample	C (wt.%)	V (kV)	d (cm)	f (mL/h)	D (nm)
SPU-1-1	12	10	10	1	770 ± 210
SPU-1-2	12	12	10	1	640 ± 170
SPU-1-3	12	15	10	1	620 ± 150
SPU-1-4	12	10	17.5	1.3	610 ± 114
SPU-2-1	10	10	17.5	1.3	600 ± 110

C — polymer concentration; V — applied voltage; d — needle-to-collector distance.
f — flow rate; D — mean fiber diameter (determined by SEM image analysis, Figs. 1 and 2).

atmosphere using the following program: 1) heating from −100 °C to 200 °C, isotherm for 2 min; 2) cooling from 200 °C to −100 °C, isotherm for 2 min; and 3) heating from −100 °C to 200 °C. Only the data from the first (first heating scan) and last steps (second heating scan) are shown in this article. SPU films and electrospun scaffold specimens with average dimensions of 20 × 5 × 0.5 mm^3 were subjected to dynamic-mechanical thermal analysis, DMTA (DMTA V Rheometric Scientific, rectangular tension/compression mode, 2 °C min^{-1} heating rate, 1.0 Hz, amplitude of 0.5%).

Water uptake of the SPU films and electrospun scaffolds were measured in triplicate (samples of 80–100 mg) after thermal equilibration (48 h) at 25 °C and 37 °C.

2.5.2. Scaffold microstructure characterization

The electrospun membranes were observed by scanning electron microscopy (SEM) using a JEOL JSM6460 LV instrument. Samples were mounted on the aluminum stub using copper double-sided adhesive tape, sputter coated with gold in a chamber evacuated to 500 mTorr, and examined with an accelerating voltage of 15 kV. The micrographs were processed and analyzed using image processing software (Image Pro Plus) to measure the fiber diameter. To obtain statistically meaningful results, at least 100 randomly selected fibers per sample were measured on SEM micrographs. The fiber diameters are expressed as the mean ± standard deviation.

3. Results and discussion

3.1. SPU synthesis and characterization

SPUs based on PEG, PLLA, and PTMC were successfully synthesized using a two-step methodology described in previous studies [21,22]. The composition of the SPU was determined using ^{1}H NMR and expressed by the mass fraction of the macrodiol block content (PEG, PLLA and PTMC). ^{1}H NMR analysis also allows for verification of the presence of carbamide hydrogens at approximately 7.8 ppm. The composition of the reaction medium and polyurethanes (both expressed as mass fraction) and molar masses of the SPUs are shown in Table 1.

3.2. Scaffold preparation and characterization

Electrospinning is a unique and versatile process to produce polymeric micro/nanofibers from polymer solutions. Although this technique is always described as a simple processing technique, it is governed by a number of parameters that affect fiber formation and structure. Fiber size and morphology are determined by a number of factors including polymer molecular weight and chemical composition, solution parameters (dielectric constant, conductivity, concentration and surface tension), processing parameters (flow rate of the solution, applied voltage, needle-to-collector distance, grounded collector characteristics), and environmental parameters (temperature, humidity) [23]. To produce defect-free nanofibers with controlled fiber diameter distribution and orientation, key parameters of the process must be precisely set and controlled.

The spinning conditions used in this work were selected after a series of screening experiments. Different polymer concentrations, mixed-solvent systems, mixing ratios and electrospinning parameters (mainly applied voltage and flow rate) were explored to ensure a cone-jet mode which is the most stable and used electrohydrodynamic mode to generate uniform nanofibers from polymeric solutions. Thus, nanofibrous scaffolds were prepared by using the parameters shown in Table 2. For comparison, classical solvent-cast films were also prepared from SPU-1 and SPU-2, and the samples are referred as SPU-1-f and SPU-2-f, respectively. The SPUs are soluble in polar solvents such as tetrahydrofuran, chloroform, dichloromethane, dimethylformamide, and fluorinated alcohols, among other common solvents. For electrospinning, solvents with high conductivity and low vapor pressure are desirable to produce electrospun fibers. Moreover, a good solvent or solvent mixture for SPU and semi-dilute concentration regime provide chain entanglements and appropriate viscosity for obtaining fibrous morphologies. In order to reach such conditions, the SPU solutions with concentration of 10–12 wt.% were prepared with a solvent mixture of DCM/DMF 60/40 by volume.

SEM analysis was performed to study the morphology of electrospun scaffolds. SPU samples displayed a typical electrospun structure of randomly oriented fibers, interconnected open macropores, and uniform pore distribution throughout the structure, which evidenced samples with high porosity (Fig. 1). The porosity values, as determined by

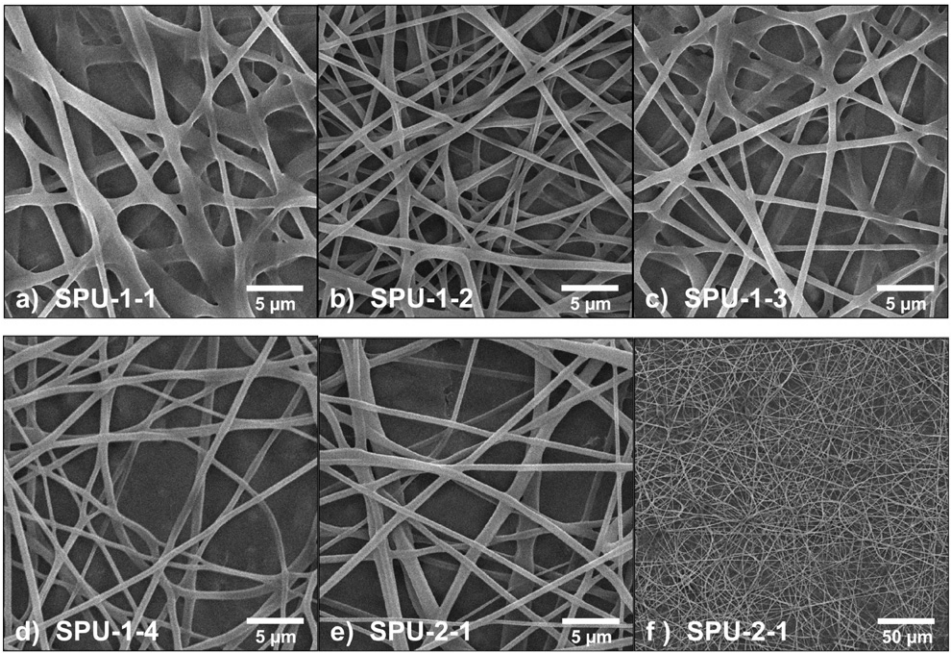

Fig. 1. SEM micrographs of SPU electrospun scaffolds obtained with different parameters (voltage, distance, flow rate and composition, Table 2).

applying image analysis methods, were in the range of 95–97%. Although this method can analyze only superficial pores without considering scaffolds with high fiber density, surprisingly it provided porosity values close to the obtained by other techniques such as liquid extrusion porosimetry (LEP) [24].

Fig. 2 shows the fiber diameter frequency distribution, whereas the mean fiber diameters (D) were found in the range of 600 to 770 nm (Table 2). The fiber diameter exhibited a unimodal distribution for all scaffolds. The effect of increasing applied voltage on fiber diameter is shown in Figs. 1a–c and 2a–c; a higher voltage to distance ratio led to thinner and more uniform fibers (samples SPU-1-1 to SPU-1-3) as a consequence of the increase of the stretching rate of the solution jets. The same effect was observed by increasing both the solution flow rate and the tip-to-collector distance (Sample SPU-1-4, Figs. 1d and 2d). Despite the composition and property differences, SPU-1 and SPU-2 could be processed under similar conditions, Figs. 1e and 2e. In Fig. 2f it is possible to compare the diameter distribution of the samples.

The dynamic mechanical properties of films and scaffolds of SPUs are shown in Fig. 3. Electrospun films are softer and less dense, presenting lower values of storage and loss modulus (E′ and E″, respectively). For a better discussion of the modulus (E′ and E″) curves, temperature ranges are demarcated in Fig. 3: β relaxation (below −50 °C), PEG and PTMC glass transition temperature range (−50 °C to −25 °C), SPU relaxation (−25 °C to 25 °C), glass transition temperature of the

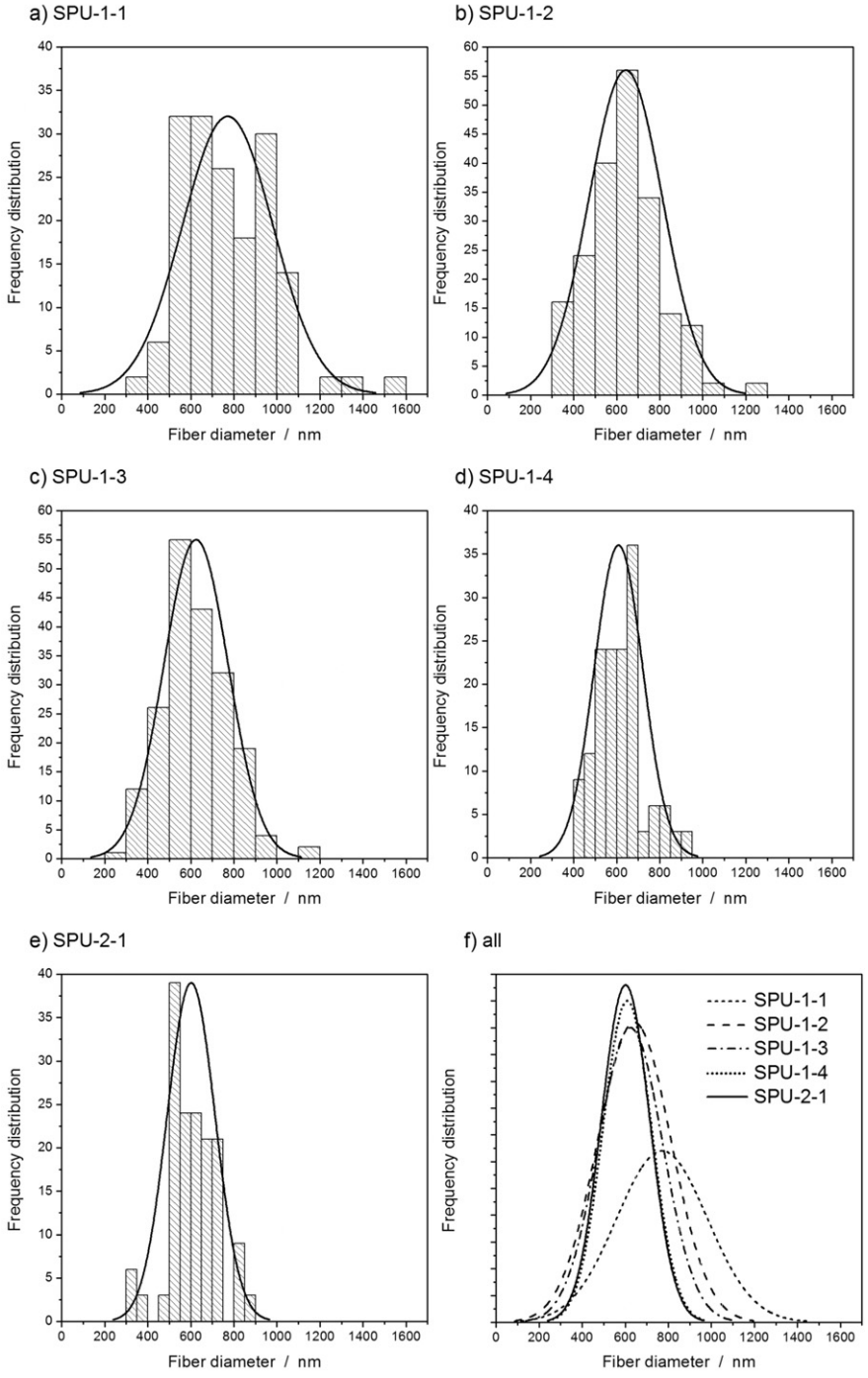

Fig. 2. Fiber diameter distributions of SPU electrospun scaffolds: a) SPU-1-1, b) SPU-1-2, c) SPU-1-3, d) SPU-1-4, e) SPU-2-1 and f) comparison of the diameter distribution of samples.

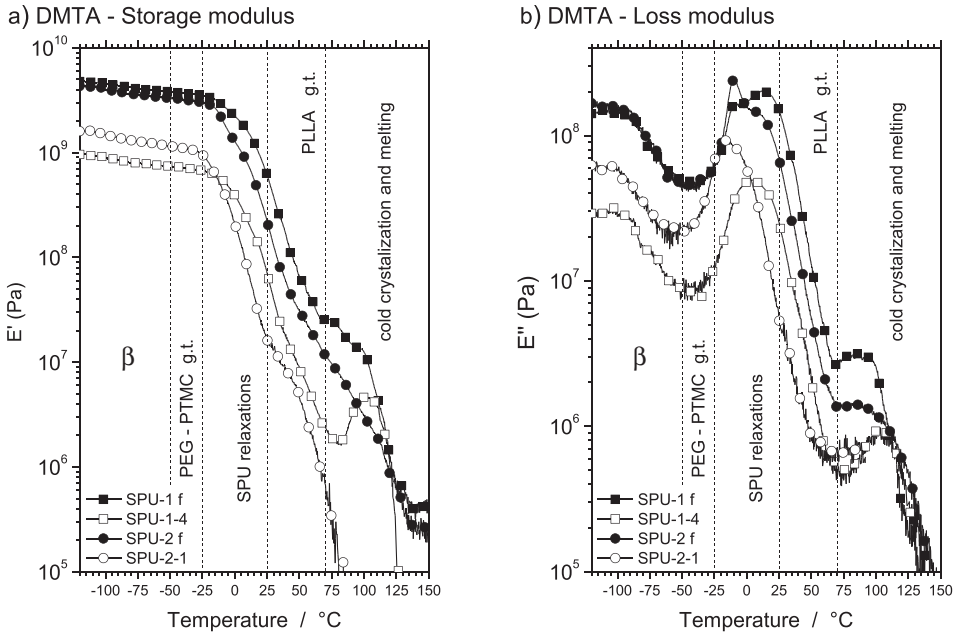

Fig. 3. Storage and loss moduli for SPU films and electrospun scaffolds.

PLLA blocks (25 °C to 75 °C), cold crystallization and melting (above 75 °C).

The β relaxation for all films and scaffolds occurs over a wide temperature range, below −50 °C (Fig. 3a) and can be understood as an overlapping of β relaxations of each block [21]. The glass transitions of PEG and PTMC were not observed in the temperature range expected for neat homopolymers (−50 °C to −25 °C), whereas the samples present wide glass transitions above in the region denoted "SPU relaxations" (−25 °C to 25 °C), as observed in both the E′ and E″ modulus curves (Fig. 3a and b). These transitions are dependent both on the composition (SPU1 and SPU-2) and on the structure (film or electrospun scaffold).

For SPU-1-f, two glass transitions are visible in the SPU relaxations range (one at approximately −10 °C and the other at approximately 15 °C, as observed in the E″ modulus curve, Fig. 3b) and are related to multicomponent phases rich in PTMC and PEG [22]. A third glass transition (better visualized in the E′ modulus curve, Fig. 3a) occurs in the 'PLLA glass transition range' (approximately 55 °C), related to a PLLA rich phase, followed by a cold crystallization at 70 °C(attributed to PLLA) and melting at approximately 95 °C (Fig. 3b). These transitions are also verified in first DSC heat curve (Fig. 4a). Although some minor differences in temperature are expected due the difference between the techniques, the DSC curves are quite complex above 70 °C, where the PLLA glass transition, cold crystallization and melting cannot be properly delimited.

Storage and loss modulus curves for the electrospun film SPU-1-4 presents a similar behavior to that of the corresponding dense film (SPU1-f), whereas the two low glass transitions in the 'SPU relaxations' range cannot be distinguished in the E″ curve (Fig. 3b, a unique Tg of approximately 5 °C is assigned), and the cold crystallization leads to a

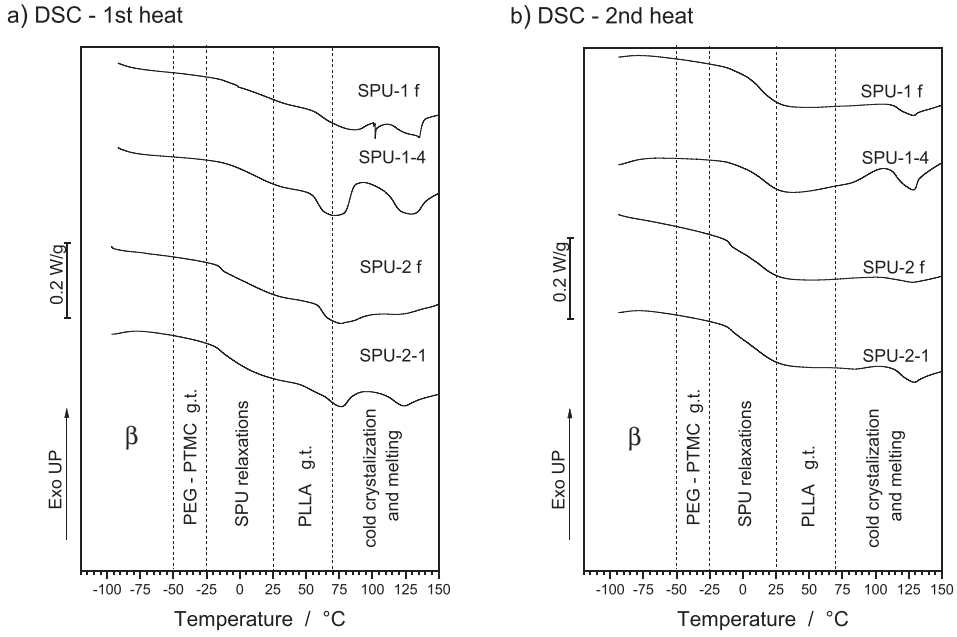

Fig. 4. First (a) and second (b) DSC heating curves for SPU films and electrospun scaffolds.

Table 3
Glass transitions, cold crystallization and melting temperatures obtained from DMTA and DSC first heat curves.

Sample	$T_{g,SPU}$ (°C) *		$T_{g,SPU}$ (°C) *		$T_{g,PLLA}$ (°C)		$T_{c,PLLA}$ (°C)		$T_{m,PLLA}$ (°C)	
	DMTA	DSC	DMTA	DSC	DMTA	DSC	DMTA	DSC	DMTA	DSC
SPU-1-f	−10	−12	15	16	55	61	70	90	90	132
SPU-1-4	5	−1		14	50	59	75	82	100	131
SPU-2-f	−10	−13	9	17	50	62	70	88	90	118
SPU-2-1	−15	−15		4	50	67	60	79	95	124

* Two glass transition events were verified for the samples in the range from −25 to 25 °C.

significant enhancement in E′ (Fig. 3a), suggesting that the crystallinity of the electrospun films is lower than that observed for the dense films. This difference can also be verified in the first DSC heat curves (Fig. 4a), in which the cold crystallization event at approximately 80 °C – 110 °C for SPU-1-4 is more expressive.

SPU-2-f presents two glass transitions at low temperature (−10 °C and 9 °C) and the events of glass transition, cold crystallization and melting approximately 50 °C, 70 °C and 110 °C, respectively. Due to the lower PLLA content, the decreases in modulus above 0 °C (after the glass transition) are greater and the cold crystallization is less expressive (E″ curves, Fig. 3b). The electrospun film SPU-2-1 presents a glass transition at a low temperature (around −15 °C) and a crystallinity lower than that of SPU-2-f. The first DSC heat curves for SPU-2 films (Fig. 4a) present the same event pattern as those of the SPU-1 films. Fig. 4b shows the second DSC heat curves, where the formation thermal history of the films was erased, reflecting the consequences of the 1st cooling over the samples.

While PLLA and PEG are semicrystalline polymers, only the PLLA component presented some degree of crystallinity, which was verified by X-Ray diffraction experiments (data shown in the Supporting information). Glass transition, crystallization and melting temperatures determined from loss modulus and the first DSC heat curves are summarized in Table 3. In the DMTA data, values were read at the peaks in E″ and the inflections in E′. In the DSC data, T_g was measured at the inflections of the first heat curves, while T_c and T_m were measured at the onset and at the peaks, respectively, of the first heat curves.

Water uptake of the SPU samples is dependent on the composition and is directly related to the PEG content, as demonstrated in a previous study on ternary SPU based on PEG, PLLA and PTMC using 2,4-toluene diisocyanate and HDI as diisocyanates [21,22]. The water uptake for SPU films and scaffolds are shown in Fig. 5 for temperatures of 25 °C and 37 °C. There is no significant difference between the SPU-1-f and SPU-2-f water uptake values, either at 25 °C (6.5 ± 0.5 and 6.1 ± 0.3, respectively) or at 37 °C (7.3 ± 0.6 and 6.9 ± 0.3, respectively). Electrospun scaffolds, however, present significantly higher values of water uptake than dense films: 55.4 ± 1.8 and 57.4 ± 2.9 for SPU-1-4 at 25 °C and 37 °C, respectively and 76.5 ± 4.2 and 78.9 ± 10.7 for SPU-2-1, at 25 °C and 37 °C, respectively. The difference in water uptake is associated with the porous structure of the electrospun scaffolds, while the difference in hydrophobicity is not significant (SPU-1-f and SPU-2-f, Fig. 5). Whereas the standard deviation does not allow differentiating the water uptake at 25 °C or 37 °C, an increasing water uptake tendency with increasing temperature is observed (entropic control).

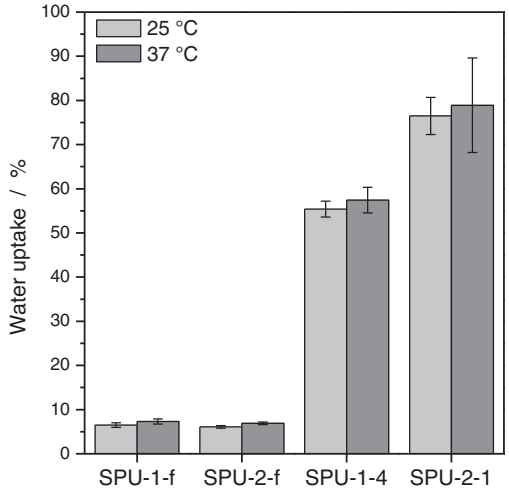

Fig. 5. Water uptake for the SPUs, measured at equilibrium at 25 °C and 37 °C.

4. Conclusions

In this work, a novel biodegradable ternary SPU based on PEG, PLLA and PTMC was successfully electrospun into engineered scaffolds. Solution properties (polymer concentration and solvent) and processing parameters (applied electric field, needle to collector distance and solution flow rate) were optimized to achieve smooth, uniform bead-free fibers. The influence of such processing parameters on the fiber morphology was investigated. Dynamic mechanical and thermal properties are dependent on both the SPU composition and the electrospun or cast scaffold characteristics, which affects the crystallinity degree. Macrodiols (PEG, PLLA, PTMC), HDI as aliphatic diisocyanate and butanediol as chain extender are components widely used in the synthesis of biodegradable SPU. Thus, the SPUs reported in this paper have interesting properties to be explored as promising candidates for soft tissue engineering, where elastomeric highly porous matrices are strongly required.

Acknowledgments

The authors acknowledge FAPESP (Process n° 2010/02098-0, 2010/17804-7 and 2011/09479-1), the Argentinean National Agency of Scientific and Technological Promotion (PICT 224 grant), and CONICET (PIP 089 grant) for financial support.

Appendix A. Supplementary data

Supplementary data to this article can be found online at http://dx.doi.org/10.1016/j.msec.2015.07.018.

References

[1] P.X. Ma, Scaffolds for tissue fabrication, Mater. Today 7 (5) (2004) 30–40, http://dx.doi.org/10.1016/S1369-7021(04)00233-0.
[2] A. Greiner, J.H. Wendorff, Electrospinning: a fascinating method for the preparation of ultrathin fiber, Angew. Chem. Int. 46 (2007) 5670–5703, http://dx.doi.org/10.1002/anie.200604646.
[3] J. Lannutti, D. Reneker, T. Ma, D. Tomasko, D. Farson, Electrospinning for tissue engineering scaffolds, Mater. Sci. Eng. C27 (2007) 504–509, http://dx.doi.org/10.1016/j.msec.2006.05.019.
[4] H. Li, Y. Xu, J. Cheng, Electrospun membranes: control of the structure and structure related applications in tissue regeneration and drug delivery, J. Mater. Chem. B 2 (2014) 5492–5510, http://dx.doi.org/10.1039/c4tb00913d.
[5] X. Wang, B. Ding, B. Li, Biomimetic electrospun nanofibrous structures for tissue engineering, Mater. Today 16 (6) (2013) 229–241, http://dx.doi.org/10.1016/j.mattod.2013.06.005.
[6] L.A. Bosworth, S. Downes (Eds.), Electrospinning for Tissue Regeneration, Woodhead Publishing, UK, 2011.
[7] S.A. Guelcher, Biodegradable polyurethanes: synthesis and applications in regenerative medicine, Tissue Eng. B 14 (2008) 3, http://dx.doi.org/10.1089/teb.2007.0133.
[8] S.A. Riboldi, N. Sadr, L. Pigini, P. Neuenschwander, M. Simonet, P. Mognol, M. Sampaolesi, G. Cossu, S. Mantero, Skeletal myogenesis on highly orientated microfibrous polyesterurethane scaffolds, J. Biomed. Mater. Res. 84A (2008) 1094–1101, http://dx.doi.org/10.1002/jbm.a.31534.
[9] J. Guan, K.L. Fujimoto, M.S. Sacks, W.R. Wagner, Preparation and characterization of highly porous, biodegradable polyurethane scaffolds for soft tissue applications, Biomaterials 26 (2005) 3961–3971, http://dx.doi.org/10.1016/j.biomaterials.2004.10.018.
[10] C. Alperin, P.W. Zandstra, K.A. Woodhouse, Polyurethane films seeded with embryonic stem cell-derived cardiomyocytes for use in cardiac tissue engineering applications, Biomaterials 26 (2005) 7377–7386, http://dx.doi.org/10.1016/j.biomaterials.2005.05.064.

[11] K.D. Kavlock, T.W. Pechar, J.O. Hollinger, S.A. Guelcher, A.S. Goldstein, Synthesis and characterization of segmented poly(esterurethane urea) elastomers for bone tissue engineering, Acta Biomater. 3 (2007) 475–484, http://dx.doi.org/10.1016/j.actbio.2007.02.001.
[12] S.A. Riboldi, M. Sampaolesi, P. Neuenschwander, G. Cossu, S. Mantero, Electrospun degradable polyesterurethane membranes: potential scaffolds for skeletal muscle tissue engineering, Biomaterials 26 (2005) 4606–4615, http://dx.doi.org/10.1016/j.biomaterials.2004.11.035.
[13] J.J. Stankus, J. Guan, K. Fujimoto, W.R. Wagner, Microintegrating smooth muscle cells into a biodegradable, elastomeric fiber matrix, Biomaterials 27 (2006) 735–744, http://dx.doi.org/10.1016/j.biomaterials.2005.06.020.
[14] S. Kidoaki, I.K. Kwon, T. Matsuda, Structural feature and mechanical property of in situ-bonded meshes of segmented polyurethane electrospun from mixed solvents, J. Biomed. Mater. Res. B Appl. Biomater. 76B (2006) 219–229, http://dx.doi.org/10.1002/jbm.b.30336.
[15] J.A. Henry, K. Burugapalli, P. Neuenschwander, A. Pandit, Structural variants of biodegradable polyesterurethane in vivo evoke a cellular and angiogenic response that is dictated by architecture, Acta Biomater. 5 (2009) 29–42, http://dx.doi.org/10.1016/j.actbio.2008.08.020.
[16] P.C. Caracciolo, A.A.A. de Queiroz, O.Z. Higa, F. Buffa, G.A. Abraham, Segmented poly(esterurethane urea)s from novel urea-diol chain extenders: synthesis, characterization and in vitro biological properties, Acta Biomater. 4 (2008) 976–988, http://dx.doi.org/10.1016/j.actbio.2008.02.016.
[17] P.C. Caracciolo, F. Buffa, G.A. Abraham, Effect of the hard segment chemistry and structure on the thermal and mechanical properties of novel biomedical segmented poly(esterurethanes), J. Mater. Sci. Mater. Med. 20 (2009) 145–155, http://dx.doi.org/10.1007/s10856-008-3561-8.
[18] P.C. Caracciolo, V. Thomas, Y.K. Vohra, F. Buffa, G.A. Abraham, Electrospinning of novel biodegradable poly(ester urethane)s and poly(ester urethane urea)s for soft tissue-engineering applications, J. Mater. Sci. Mater. Med. 20 (10) (2009) 2129–2137, http://dx.doi.org/10.1007/s10856-009-3768-3.
[19] P.C. Caracciolo, F. Buffa, V. Thomas, Y.K. Vohra, G.A. Abraham, Biodegradable polyurethanes: comparative study of electrospun scaffolds and films, J. Appl. Polym. Sci. 121 (6) (2011) 3292–3299, http://dx.doi.org/10.1002/app.33855.
[20] R.B. Trinca, M.I. Felisberti, Influence of the synthesis conditions on the structural and thermal properties of poly(L-lactide)-b-poly(ethylene glycol)-b-poly(L-lactide), J. Appl. Polym. Sci. 131 (13) (2014) 40419, http://dx.doi.org/10.1002/app.40419.
[21] R.B. Trinca, M.I. Felisberti, Segmented polyurethanes based on poly(L-lactide), poly(ethylene glycol) and poly(trimethylene carbonate): physico-chemical properties and morphology, Eur. Polym. J. 62 (2015) 77–86, http://dx.doi.org/10.1016/j.eurpolymj.2014.11.008.
[22] R.B. Trinca, M.I. Felisberti, Effect of diisocyanates and chain extenders on the physical-chemical properties and morphology of multicomponent segmented polyurethanes based on poly(L-lactide), poly(ethylene glycol) and poly(trimethylene carbonate), Int. Polym. (2015) http://dx.doi.org/10.1002/pi.4920 (Article first published online: 21 APR 2015).
[23] N. Bhardwaj, S.C. Kundu, Electrospinning: a fascinating fiber fabrication technique, Biotechnol. Adv. 28 (2010) 325, http://dx.doi.org/10.1016/j.biotechadv.2010.01.004.
[24] P. Cortez Tornello, P.C. Caracciolo, T.R. Cuadrado, G.A. Abraham, Structural characterization of electrospun micro/nanofibrous scaffolds by liquid extrusion porosimetry: a comparison with other techniques, Mater. Sci. Eng. C 41 (2014) 335–342, http://dx.doi.org/10.1016/j.msec.2014.04.065.